^{99m}Tc generator using molybdenum nanoparticles

Naruto Takahashi[1,2] · **Mamoru Fujiwara**[1] · **Maki Kurosawa**[1] · **Masoto Tamura**[1] · **Yoshiaki Kosuge**[2] · **Takumi Kubota**[3] · **Naoya Abe**[3] · **Toshiharu Takahashi**[3]

Abstract
A novel ^{99m}Tc generator was proposed herein using nanoparticles consisting of natural Mo and an alumina column for ^{99m}Tc scintigraphy. ^{99m}Tc was obtained from ^{99}Mo decay produced via the irradiation of nanoparticles consisting of natural Mo with bremsstrahlung γ-rays using a 30 MeV electron beam. The irradiated nanoparticles were placed in an alumina column, and the ^{99m}Tc daughter from ^{99}Mo decay was separated by the removal of the ion-exchanged water or saline. This separation procedure was repeated at regular intervals for one week. The maximum separation yield of ^{99m}Tc was $14.4 \pm 0.7\%$, which is sufficiently high to produce ^{99m}Tc suitable for medical use.

Introduction

Tc-99 m is used in nuclear medicine to diagnose diseases of the bone, heart, lung, liver, and kidney. In particular, ^{99m}Tc-methylene diphosphonic acid (MDP) [1] and ^{99m}Tc-hydroxy methylene phosphonic acid (HMDP) [2] are commonly used to detect bone disease with an annual use of about 1.6×10^8 MBq (Japan Isotope Society statistical data 2020) [3] every year in Japan. Moreover, ^{99m}Tc-human serum albumin (HAS)-diethylene triamine pentaacetic acid [4] and ^{99m}Tc-macro-aggregated human serum albumin (MAA) [5] are used to treat heart and lung diseases at consumption rates with an annual use of about 7.6×10^7 MBq. In addition, 4.4×10^7 MBq is used for other purposes. Therefore, a total of 2.8×10^8 MBq of ^{99m}Tc is used every year for nuclear medicine-based diagnoses. The global consumption of ^{99}Mo in 2016 was estimated at approximately 1.7×10^{10} MBq, half of which was consumed in the United States [6].

Currently, ^{99m}Tc is supplied by a highly compact generator with carrier-free ^{99}Mo as the parent nuclide adsorbed onto an alumina column [7]. Mo-99 is produced in a nuclear reactor [8] and chemically separated from the fission products of uranium. However, supply shortages of ^{99}Mo/^{99m}Tc are emerging as an increasingly common issue because of reactor malfunctions and international transportation accidents and backlogs. Furthermore, it is likely that the performance of nuclear reactors will deteriorate over time, resulting in additional supply shortages [9]. Many reports [10–12] have proposed the replacement of aging nuclear reactors for the production of ^{99}Mo.

^{99}Mo production through ^{98}Mo(n, γ)^{99}Mo [13], ^{100}Mo (p, d)^{99}Mo [14], and ^{100}Mo (γ, n)^{99}Mo reactions [15, 16] using an accelerator has been reported as an alternative to fission. In this work, we also utilized this photoactivation mechanism. We confirmed that an electron LINAC as is typically used in nuclear medicine [17], can be used to produce ^{99}Mo. However, it is not possible to use the current ^{99m}Tc generator to ensure adherence of Mo to the alumina column because a large amount of target Mo (stable isotope Mo) is contained in the mixture of ^{99}Mo produced using the electron accelerator. Therefore, the generation of ^{99}Mo by photoactivation does not carrier-free ^{99}Mo.

The small adsorption capacity of alumina can be a significant concern, as the amount of absorbed Mo is typically in the range of 10 mg/g of alumina. For example, to

✉ Naruto Takahashi
naruhito102@gmail.com

1 Research Center for Nuclear Physics, Osaka University, Mihogaoka 10-1, Ibaraki, Osaka 567-0047, Japan

2 Kyoto Medical Technology Co, Kyoto 606-8225, Japan

3 Institute for Integral Radiation and Nuclear Science, Kyoto University, Kumatori, Osaka 590-0494, Japan

produce 30 GBq of ^{99}Mo via photonuclear reaction with 30 MeV photons and a 1 mA electron beam, 10 g of natural Mo should be irradiated for 10 h. Concerning the aforementioned rate, 1 kg of alumina would be needed for 10 g of the Mo target. Recent advances in the understanding of Mo adsorption to alumina are promising [18, 19], but the associated strategies have not been implemented thus far.

Equipment was developed to separate ^{99m}Tc via solvent extraction using methyl ethyl ketone [20]. This method uses ^{nat}MoO$_3$ as a target to separate ^{99m}Tc from ^{99}Mo produced via ^{98}Mo(n, γ)^{99}Mo, ^{100}Mo(p, d)^{99}Mo, or ^{100}Mo(γ, n)^{99}Mo reactions using a two-tank separator. After ^{99m}Tc separation, it was reacted with MDP and applied to obtain a clear bone scintigram of a mouse [21].

Herein, we report a simple method for separating ^{99m}Tc from ^{99}Mo/^{99m}Tc using Mo nanoparticles. The use of nanoparticles leads to the possibility of fixating the mother nuclide ^{99}Mo mechanically instead of chemisorption, therefore circumventing the use of large amounts of alumina. However, under this conditions the daughter ^{99m}Tc can only be eluted from a column when ^{99}Mo nuclei are recoiled out of the nanoparticles. Russian researchers have calculated the rate at which ^{99}Mo recoils in the ^{100}Mo(γ, n) ^{99}Mo reaction using Mo nanoparticles that reach the particle surface has been calculated by Starovoitova et al. [22]. We conducted the first experiment to separate ^{99m}Tc from the recoiled ^{99}Mo/^{99m}Tc using a method that is simpler than solvent extraction, which employs commercially available ^{99}Mo/^{99m}Tc generator systems. Herein, Mo nanoparticles with diameters of several tens of nanometers and an alumina column were used.

Experimental

The production of ^{99}Mo via $^{nat.}$Mo(γ, n) ^{99}Mo reaction was conducted at the electron LINAC facility at the Institute for Integrated Radiation and Nuclear Science, Kyoto University. Mo nanoparticles used therein possessed a commercially available natural isotope composition and the size was determined by x-ray diffraction. Metal Mo (100 mg) and MoO$_3$ with the particle sizes of 35–45 and 13–80 nm, respectively, were used as powders or suspended in water. The samples used in the following experiments are presented in Table 1. Each target was sealed in a quartz tube and irradiated with bremsstrahlung γ-rays emitted from a 2-mm-thick Pt bombarded with 100 µA and 30 MeV electrons. A total of 2 MBq of ^{99}Mo was obtained from these irradiations. After irradiation, the energy spectra of γ-rays from each target and the separated ^{99m}Tc solution were measured using a Ge detector. For the detector used for the gamma-ray measurement, energy calibration and detection efficiency were obtained in

Table 1 Sample descriptions and experimental conditions

| No	Sample	Particle size	Irradiated condition	Separated condition
1a	Mo metal	35–45 nm	dry powder	ion-exchanged water
1b	Mo metal	35–45 nm	suspended in saline	ion-exchanged water
2a	MoO$_3$	13–80 nm	dry powder	ion-exchanged water
2b	MoO$_3$	13–80 nm	suspended in ion-exchanged water	ion-exchanged water
2c	MoO$_3$	13–80 nm	suspended in saline	saline

Fig. 1 Photograph of the novel ^{99m}Tc generator with an alumina column. Gamma-irradiated Mo nanoparticles were set on top of the column. **a** Saline, **b** MoO$_3$ nanoparticles, **c** Alumina, and d:Separated ^{99m}Tc solution
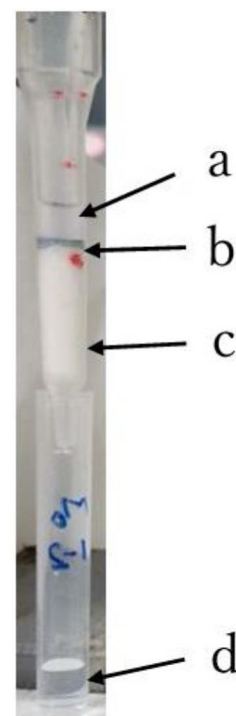
advance using standard sources. Furthermore, geometrical correction was performed by using Monte Carlo simulation.

As shown in Fig. 1, the irradiated Mo nanoparticles were added to a column filled with 1 cm^3 of activated alumina in ion-exchanged water or saline. The generator vessel was made of polyethylene and the column filled with alumina had a diameter of 5 mm, a wall thickness of 1.5 mm and an overall height of 12 cm. For ^{99m}Tc separation, 2 mL of ion-exchanged water or saline was passed through the column. As shown in Fig. 1, the separated ^{99m}Tc solution was collected in a polyethylene tube and measured separately from the column with a Ge detector. The chemical separation and γ-ray measurement were repeated at regular intervals for one week, and the time dependence of radioactivity in the

Fig. 2 Gamma-ray spectra of **a** MoO$_3$ nanoparticle powder irradiated by Bremsstrahlung rays and **b** ^{99m}Tc solution separated from MoO$_3$
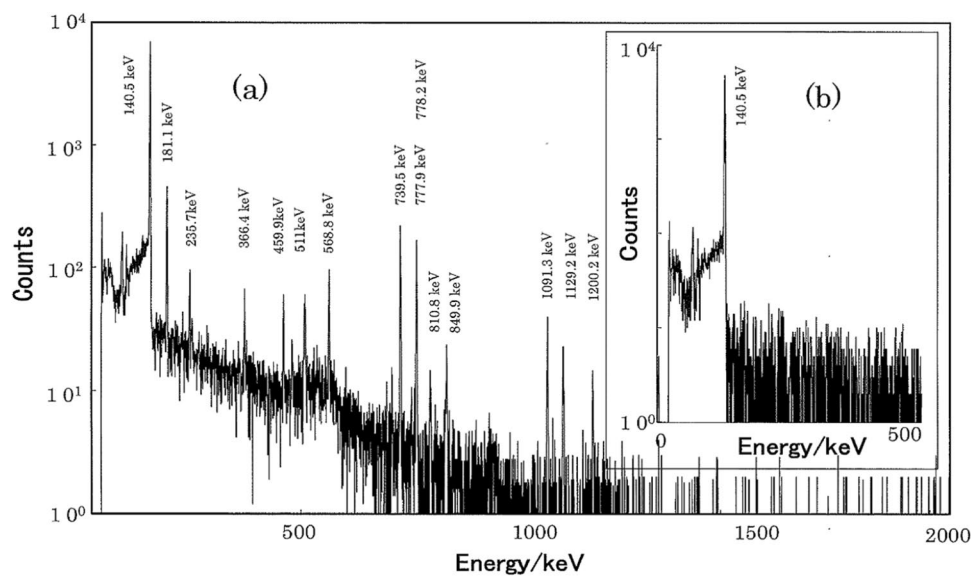

column and the radioactivity-separated ^{99m}Tc solution were measured. In addition, the nanoparticles were imaged using an electron microscope to investigate their size and shape.

Results and discussion

Figure 2 shows the γ-ray spectra of MoO$_3$ after 3 h of irradiation and the effluent solution obtained by flowing ion-exchanged water through the MoO$_3$ nanoparticles in the aluminum column. A 140.5 keV peak originated from ^{99m}Tc was observed. In addition, peaks were observed at 181.1, 366.4, 739.5, and 777.9 keV corresponding to ^{99}Mo; the peak at 235.7 keV was attributed to ^{95m}Nb; 568.8 keV, 765.8 keV, 778.2 keV, 810.8 keV, and 1200.2 keV peaks from ^{96}Nb. Figure 2b shows the γ-ray spectrum of the ^{99m}Tc solution separated from MoO3. Only the 140.5 keV peak from ^{99m}Tc was observed, indicating that all ^{99}Mo, parent nuclei, and side reaction products of ^{95m}Nb and ^{96}Nb were adsorbed onto the column. The percentage of radioisotopes remaining on the column was ^{99}Mo > 99.5%, ^{95m}Nb > 97% and ^{96}Nb > 98%, respectively.

Figure 3 shows the decay curve of the 181.1 keV γ-ray in the effluent solution. A solid line was obtained through the least square fitting of the observed data. A linear fit was obtained through least square fitting of the observed data on a logarithmic scale, yielding a calculated half-life was 66.0 ± 0.6 h, being in good coincidence with the literature value 65.9 h. The radioactivity of ^{99m}Tc in the column before elution and in the eluate was determined at regular time intervals. Figure 4 shows the recovery rate of ^{99m}Tc from MoO$_3$ as a function of time. In Fig. 4, the horizontal axis represents the elapsed time from the end of bombardment. The recovery was calculated at the time the radioactivity of
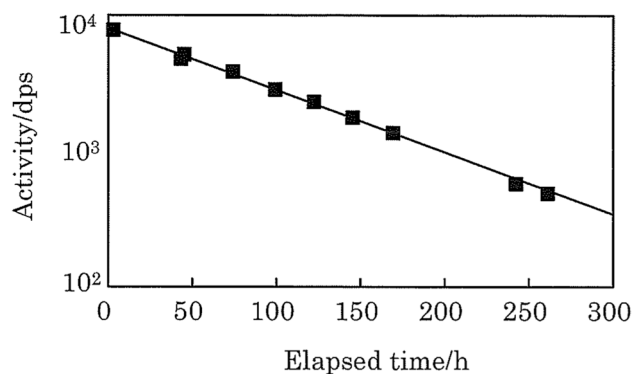
Fig. 3 Decay curve of the 181.1 keV photopeak. Solid line was derived from the least squares fit of the observed data. Error bars of the data are hidden inside square
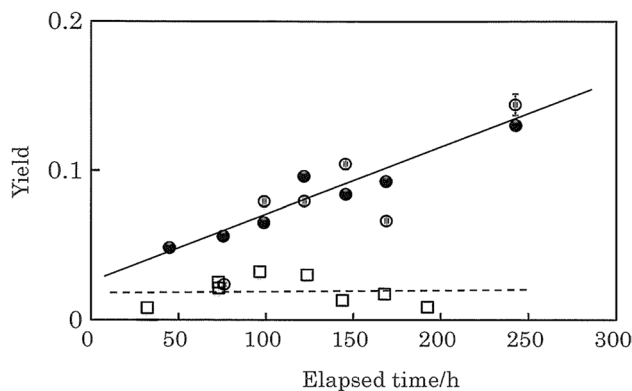
Fig. 4 Recovery rate of ^{99m}Tc from the ^{99}Mo/^{99m}Tc produced by the irradiated MoO$_3$ nanoparticle. Open and closed circles are MoO$_3$ nanoparticle suspended in ion-exchanged water and saline, respectively. Rectangle is MoO$_3$ nanoparticle powder

^{99m}Tc in the column was measured. The yield was defined as the ratio of ^{99m}Tc activity in the separated solution to that retained in the column. Data are shown for irradiation with powder alone, nanoparticles suspended in ion-exchanged water, and nanoparticles suspended in physiological saline. ^{99m}Tc yield was observed as a function of time for all samples. The recovery yields of ^{99m}Tc obtained in these experiments are listed in Table 2. The yields for Mo metal were significantly lower than those for MoO$_3$, whereas those for MoO$_3$ irradiated in aqueous conditions were higher than those under dry conditions.

Even while maintaining a constant MoO$_3$ content, the separation yield of ^{99m}Tc for nanoparticles suspended in an aqueous solution was higher than that for the powdered form. This is because the individual particles diffused in the solvent and did not stick to each other during irradiation. However, if the particles were not first suspended in the solvent, they grew larger owing to gamma ray irradiation, and very few ^{99}Mo/^{99m}Tc reached particle surface.

Considering the recovery rates of ^{99m}Tc in Mo and MO$_3$ nanoparticles, the yield of MoO$_3$ was approximately 20 times higher than that of Mo metal, primarily owing the nanoparticle shape. Figure 5 shows electron micrographs of the Mo and MoO$_3$ nanoparticles. The Mo metal was spherical with a size of approximately 100 nm, while MoO$_3$

was orthorhombic with a particle size of approximately 10 μm. While the recoil rate from the small size of particles is expected to increase owing to the large specific surface area, the results revealed that MoO$_3$ with a large particle size exhibits a higher yield.

Dikiy et al. calculated the escape fraction of ^{99}Mo produced via the ^{100}Mo (γ, n) ^{99}Mo reaction with photons possessing an end point energy of 30 MeV [23] and obtained values of 0.06 and 0.08 for 70 nm Mo and MoO$_3$, respectively. The experimental results presented herein for ^{99m}Tc yield was 0.003 ± 0.001 for Mo, which is approximately 1/20 of the simulation results reported by Dikiny et al. This indicates that ^{99}Mo recoiled from the inside of the nanoparticles to the surface. However, the probability of being trapped in the aqueous solution was low. For MoO$_3$, the ratio of ^{99}Mo trapped as ^{99m}Tc was 0.05 ± 0.006, yielding a trap efficiency of 0.6, which is significantly greater than that of Mo metal. Based on these experimental results, it seems that ^{99m}Tc can be separated with a higher yield by using even smaller MoO$_3$ nanoparticles and performing gamma-ray irradiation in a state in which the particles do not stick together.

The separation of ^{99m}Tc was repeated several times at intervals of approximately one day. The yield increased for the MoO$_3$ nanoparticles as a function of time, and the maximum separation yield of ^{99m}Tc was 14.4 ± 0.7% (Fig. 4).

Table 2 Recovery yields of ^{99m}Tc

No	Sample	Irradiated condition	Separated condition	Min. yield (%)	Max. yield (%)
1a	Mo metal	dry powder	ion-exchanged water	0.08 ± 0.01	0.29 ± 0.28
1b	Mo metal	suspended in saline	ion-exchanged water	0.05 ± 0.03	0.94 ± 0.21
2a	MoO$_3$	dry powder	ion-exchanged water	0.81 ± 0.03	3.2 ± 0.1
2b	MoO$_3$	suspended in ion-exchanged water	ion-exchanged water	2.4 ± 0.1	14.4 ± 0.7
2c	MoO$_3$	suspended in saline	saline	4.8 ± 0.1	13.0 ± 0.7
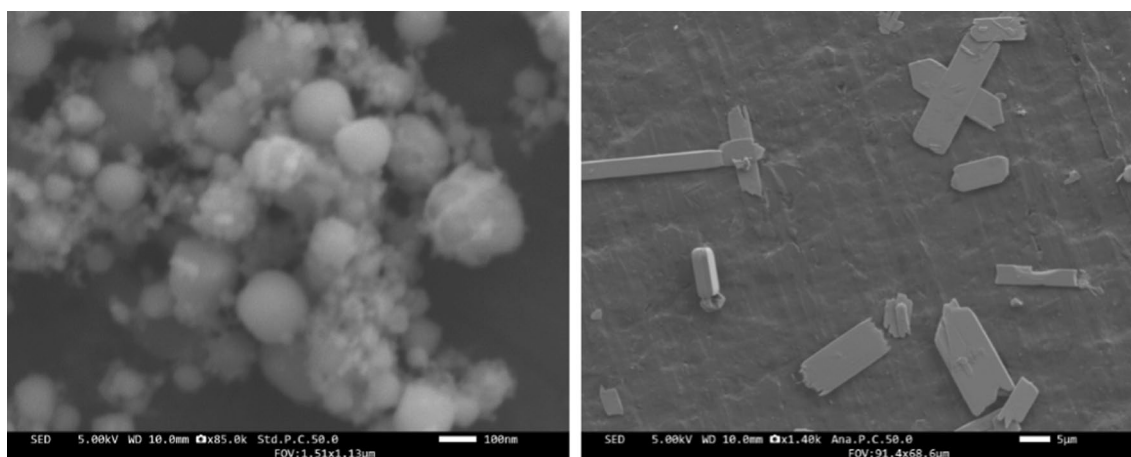
Fig. 5 Electron microscopy image of the prepared nanoparticles. (left) Mo nanoparticles with a particle size of 10~250 nm and (right) MoO$_3$ nanoparticles with a size of 2–10 μm

This indicated that the Mo nanoparticles acted as a ^{99m}Tc generator.

Conclusion

A novel ^{99m}Tc generator employing Mo nanoparticles and an alumina column was proposed. ^{99}Mo was produced via a photonuclear reaction using naturally composed Mo metal and MoO$_3$ nanoparticles as targets. The irradiated nanoparticles were poured into an alumina column, and ^{99m}Tc was separated at regular intervals using ion-exchanged water and saline. The nanoparticles suspended in the ion-exchanged water provided a higher ^{99m}Tc yield compared with the powdered nanoparticles. However, no difference in the ^{99m}Tc yield was observed between ion-exchanged water and saline. The maximum separation ^{99m}Tc yield was $14.4 \pm 0.7\%$.

Declarations

References

1. Delaloye B, Delaloye-Bischof A, Dudczak R, Koppenhagen K, Mata F, Penafiel A, Maul FD, Pasquier J (1985) Clinical comparison of ^{99m}Tc-HMDP and ^{99m}Tc-MDP. Eur J Nucl Med 11:182–185
2. Alam MS, Takeuchi R, Kasagi K, Misaki T, Miyamoto S, Iida Y, Hidaka A, Konishi N (1997) Value of combined technetium-99m hydroxy methylene diphosphonate and thallium-201 imaging in detecting bone metastases from thyroid carcinoma. Thyroid 7:705–712
3. Japan Radioisotope Association (2020) Statics on the distribution of radioisotopes in Japan 2020 (in Japanese). Japan Radioisotope Association Tokyo
4. Mabuchi N, Hamada T, Ishikawa K, Sakashita T, Shibata Y et al (1983) Clinical comparison of ^{99m}Tc diethylenetriamine pentaacetic acid-human serum albumin (^{99m}Tc-HAS-D) and ^{99m}Tc-human serum albumin (^{99m}Tc-HAS) for cardiac blood pool imaging. Radioisotopes 37(7):380–386
5. Gandric S, Sonik B, Subramanyam P, Palanisway S (2013) ^{99m}Tc-MAA scintigraphy-indications other than pulmonary embolism-a pictorial essay. J Nucl Med 54:1263–1269
6. Committee on State of Molybdenum-99 Production and utilization and progress toward eliminating use of highly enriched uranium nuclear and radiation studies board division on earth and life studies (2016) Molybdenum-99/Technetium-99m supply National Academies of Sciencies·Engineering·Medicine 187-200 2016
7. Fujita Y, Seki M, Sano T, Fujihara Y, Kitagawa T et al (2021) Effect on ^{99}Mo-adsorption/^{99m}Tc-elution properties of alumina with different surface structures. J Radioanal Nucl Chem 327:1355–1363
8. IAEA-TECDOC-1065 (1999) Production technologies of molybdenum-99 and technetium-99m IEEA Vienna
9. htp:// JSNM.org./archives/2827/ Technetium product supply Q & A Japanese Society of Nuclear Medicine
10. Ruth T (2020) The shortage of Tc-99m. Annu Rev Nucl Part Sci 20:77–94
11. IAEA radioisotopes and radiopharmaceutical reports (2019) Cyclotron based production of technetium-99m IAEA Vienna
12. IAEA (1999)-TECDOC-1066 Production technologies for molybdenum-99 and technetium-99m IAEA Vienna
13. Nagai Y, an Hatsukawa Y, (2009) Production of ^{99}Mo for nuclear medicine by ^{100}Mo($n,2n$)^{99}Mo. J Phys Soc JP 78:033201–033204
14. Nakai K, Takahashi N, Hatazawa J, Shinohara A, Hayashi Y, Ikeda H, Kanai Y, Watabe T, Fukuda M, Hatanaka K (2014) Feasibility studies towards future self-sufficient supply of the ^{99}Mo-^{99m}Tc isotopes with Japanese accelerators. Proc Jpn Acad B90:413–421
15. Kikunaga H, (2015) presentation/part2/Med Sci Kickoff Sympo RI production via photonuclear reaction with electron linear accelerator (in Japanese) http://www.rcnp.osaka-u.ac.jp/MedSciSympo2015Kikunagapdf
16. Inagaki M, Sekimoto S, Tadokoro T, Ueno Y, Kani Y, Ohtsuki T (2020) Production of ^{99}Mo/^{99m}Tc by photonuclear reaction using a ^{nat}MoO$_3$ target. J Radioanal Nucl Chem 324:681–686
17. Takeda T, Fujiwara M, Kurosawa M, Takahashi N, Tamura M, Fujikawa Y, Suzuki N, Abe N, Kubota T, Takahashi T (2018) ^{99m}Tc production via the (γ, n) reaction on natural Mo. J Radional Nucl Chem 318:811–821
18. Tanase M, Tatenuma K, Ishikawa K, Kurosawa K, Nishino M, Hasegawa Y (1997) A ^{99m}Tc generator using a new inorganic polymer adsorbent for (n, γ)^{99}Mo. Appl Radiat Isot 48:607–611
19. IAEA (1995) Alternative technologies for ^{99}Tcm generators. TEC-DOC-852 4:11–15
20. Takahashi N (2020) Technetiun-99m separation system and technetium-99m separation method. International patent PCT/JP2020/007936
21. Takahashi N, Nakai K, Shinohara A, Hatazawa J, Nakamura M, Fukuda M, Hatanaka K, Morikawa Y, Kobayashi M, Yamamoto (2012) Production of ^{99}Mo-^{99m}Tc by using spallation neutron. 2012 SNM annual meeting Miami
22. Starovoitova VN, Tchelidze L, Wells DP (2014) Production of medical radioisotopes with linear accelerators. Appl Radiat Isot 85:39–44
23. Dikiy NP, Dovbnya AN, Fedorchenko DV, Khazhmuradov MA (2016) GEANT 4 simulation of ^{99}Mo photonuclear production in nanoparticles. Appl Radiat Isot 114:7–13

Publisher's Note Springer Nature remains neutral with regard to jurisdictional claims in published maps and institutional affiliations.